Methods for Clinical Evaluation of Noise Reduction Techniques in Abdominopelvic CT[1]

Eric C. Ehman, MD
Lifeng Yu, PhD
Armando Manduca, PhD
Amy K. Hara, MD
Maria M. Shiung, BA
Dayna Jondal, BA
David S. Lake, MS
Robert G. Paden, MS
Daniel J. Blezek, PhD
Michael R. Bruesewitz, RT
Cynthia H. McCollough, PhD
David M. Hough, MD
Joel G. Fletcher, MD

Most noise reduction methods involve nonlinear processes, and objective evaluation of image quality can be challenging, since image noise cannot be fully characterized on the sole basis of the noise level at computed tomography (CT). Noise spatial correlation (or noise texture) is closely related to the detection and characterization of low-contrast objects and may be quantified by analyzing the noise power spectrum. High-contrast spatial resolution can be measured using the modulation transfer function and section sensitivity profile and is generally unaffected by noise reduction. Detectability of low-contrast lesions can be evaluated subjectively at varying dose levels using phantoms containing low-contrast objects. Clinical applications with inherent high-contrast abnormalities (eg, CT for renal calculi, CT enterography) permit larger dose reductions with denoising techniques. In low-contrast tasks such as detection of metastases in solid organs, dose reduction is substantially more limited by loss of lesion conspicuity due to loss of low-contrast spatial resolution and coarsening of noise texture. Existing noise reduction strategies for dose reduction have a substantial impact on lowering the radiation dose at CT. To preserve the diagnostic benefit of CT examination, thoughtful utilization of these strategies must be based on the inherent lesion-to-background contrast and the anatomy of interest. The authors provide an overview of existing noise reduction strategies for low-dose abdominopelvic CT, including analytic reconstruction, image and projection space denoising, and iterative reconstruction; review qualitative and quantitative tools for evaluating these strategies; and discuss the strengths and limitations of individual noise reduction methods.

Abbreviations: ACR = American College of Radiology, aNLM = adaptive nonlocal means (denoising method), ASIR = adaptive statistical iterative reconstruction, $CTDI_{vol}$ = volume CT dose index, FBP = filtered backprojection, MBIR = model-based iterative reconstruction, MTF = modulation transfer function, NPS = noise power spectrum, SAFIRE = sinogram-affirmed iterative reconstruction, SSP = section sensitivity profile, 3D = three-dimensional

RadioGraphics 2014; 34:849–862

Published online 10.1148/rg.344135128

Content Codes: CT GI PH QA

[1]From the Departments of Radiology (E.C.E., L.Y., A.M., M.M.S., D.J., M.R.B., C.H.M., D.M.H., J.G.F.) and Biomedical Engineering (D.S.L., D.J.B.), Mayo Clinic, 200 First St SW, Rochester, MN 55905; and Department of Radiology, Mayo Clinic, Scottsdale, Ariz (A.K.H., R.G.P.). Presented as an education exhibit at the 2012 RSNA Annual Meeting. Received June 12, 2013; revision requested August 5 and received September 20; accepted October 7. For this journal-based SA-CME activity, the authors A.M., A.K.H., D.J.B., C.H.M., and J.G.F. have disclosed financial relationships (see p 861); the other authors, editor, and reviewers have no relevant relationships to disclose. **Address correspondence to** J.G.F. (e-mail: *fletcher.joel@mayo.edu*).

SA-CME LEARNING OBJECTIVES

After completing this journal-based SA-CME activity, participants will be able to:

- Describe existing noise reduction strategies for low-dose CT, including filtered backprojection, image and projection space denoising, and iterative reconstruction.
- List quantitative and qualitative tools and metrics for evaluating these noise reduction strategies.
- Discuss the strengths and limitations of individual noise reduction techniques.

See www.rsna.org/education/search/RG.

TEACHING POINTS

See last page

Introduction

There has been a rapid increase in the use of computed tomography (CT) in recent years. An estimated 62 million–plus CT examinations were performed in the United States in 2006 (1), with the number of CT examinations for some health systems tripling between 1996 and 2010 (2). Radiation from CT makes up a large proportion of total medical radiation (1), and there is concern regarding the long-term effects of radiation exposure (3–6); consequently, there has been significant interest in reducing radiation dose to patients during CT examinations.

Radiologists seek to maximize the benefit of CT by performing only those examinations that are medically justified and optimized, thereby accomplishing the diagnostic task while minimizing the radiation dose (7). The radiation dose necessary to deliver needed patient benefit can be reduced by *(a)* limiting unnecessary examinations and superfluous acquisitions (eg, imaging during unnecessary phases of contrast material enhancement or imaging of irrelevant body regions),

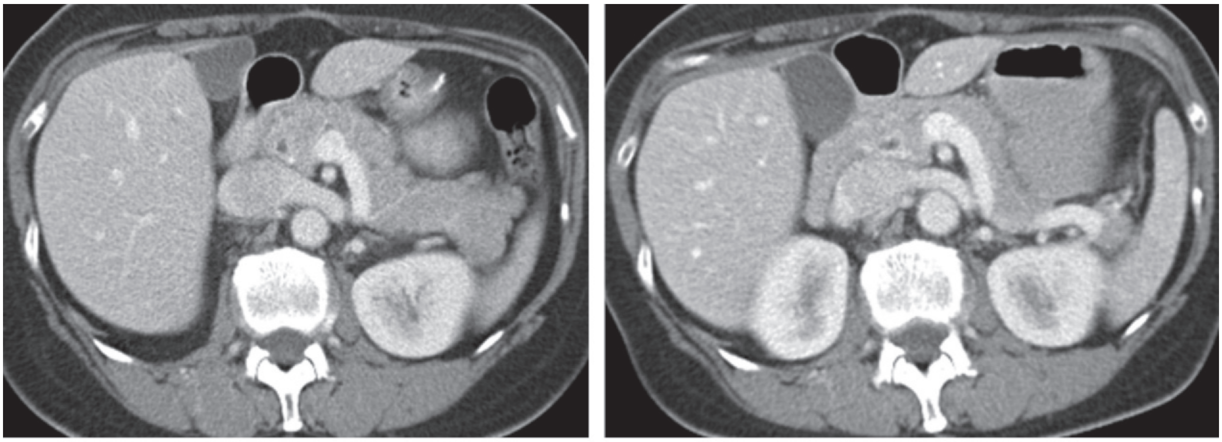

a. b.

Figure 1. Radiation dose and noise reduction using analytic FBP and standard reconstruction kernels in a 64-year-old woman with a history of gastrointestinal stromal tumor. **(a)** CT image obtained at an automatic exposure control tube current setting of 240 quality reference mAs. **(b)** CT image obtained with 33% dose reduction by lowering the automatic exposure control tube current setting to 200 quality reference mAs and using a smoother reconstruction kernel, which reduces image noise and sharpness. There is little change in overall image noise and quality (cf **a**).

(b) optimizing CT acquisition parameters (ie, lowering the milliampere-seconds or kilovolt peak), *(c)* routinely using size adaptation techniques such as automatic exposure control, or *(d)* improving the postprocessing and reconstruction of CT images (8–10). For any given CT examination, the lower the radiation dose, the noisier the resulting image. Dose reduction is limited primarily by the radiologist's ability to accomplish the diagnostic task for which a CT examination is ordered. For lower-dose examinations, the ability to detect relevant disease on noisier images will depend on many factors, including lesion size, lesion contrast compared with that of the surrounding tissues, and image noise and sharpness. By applying data processing and image reconstruction techniques that decrease image noise while maintaining spatial resolution, it is possible to improve the quality and diagnostic value of inherently noisy low-dose CT images.

In this article, we review existing noise reduction strategies for low-dose abdominopelvic CT, including analytic reconstruction, image and projection space denoising, and iterative reconstruction; describe quantitative and qualitative tools and metrics for evaluating these strategies; and discuss the strengths and limitations of individual noise reduction techniques.

Noise Reduction Techniques

Noise reduction can occur at various stages of the CT imaging process. In conventional analytic filtered backprojection (FBP)–based reconstruction, a smooth filter is typically applied to control noise. Some CT vendors offer a selection of sharper and smoother kernels for abdominal imaging, and simply choosing a smoother kernel can reduce image noise (Fig 1) (11). For many diagnostic tasks in abdominal CT, noisy low-dose images can be readily interpreted by radiologists without any adverse effects on diagnostic performance (12–16). Noise reduction can also occur in projection space prior to reconstruction (17–19) or in image space (ie, on CT images) after reconstruction (20,21). Recently, iterative reconstruction, an iterative process performed between projection space and image space to optimize an objective function and achieve "convergence," has become a popular choice for reducing image noise and improving image quality (see "Iterative Reconstruction") (22–25). Figure 2 shows the points during the CT image reconstruction process at which analytic FBP reconstruction, projection space denoising, image space denoising, and iterative reconstruction are applied.

Teaching Point

Image Space Denoising

Image space denoising is the process of filtering the reconstructed images to reduce noise (20,26,27). Image space denoising filters are available on some commercial scanners or, more commonly, as third-party products, and filter design varies. To maintain information about small structures in the image, this type of filter is typically nonlinear and designed to be adaptive to sharp edges (ie, to remove high-frequency noise only when there is no structural edge). Loss of edge detail and spatial resolution may still occur if the filter is not appropriately designed or if the filter strength is not carefully controlled, which may result in reduced detectability of low-contrast lesions. Figure 3 demonstrates loss of lesion con-

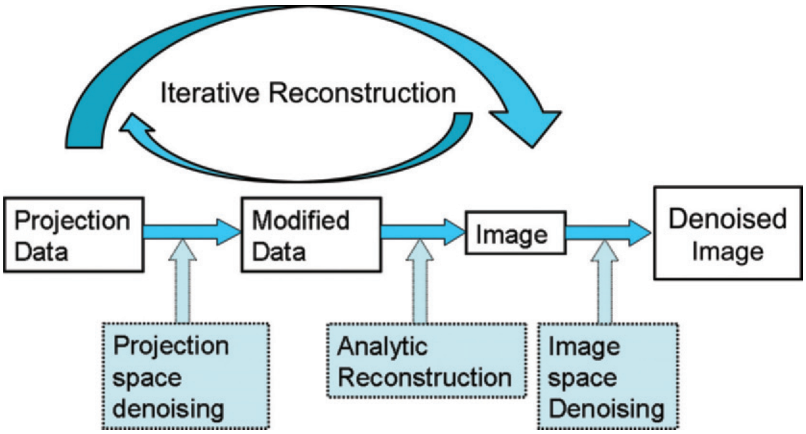

Figure 2. Schematic illustrates the points during the CT image reconstruction process at which noise reduction techniques are applied. Projection space denoising, analytic FBP (standard reconstruction kernels), and image space denoising are applied during or after analytic reconstruction. Iterative reconstruction represents an alternative pathway to image reconstruction that optimizes an objective function by using an iterative loop between projection and image data.

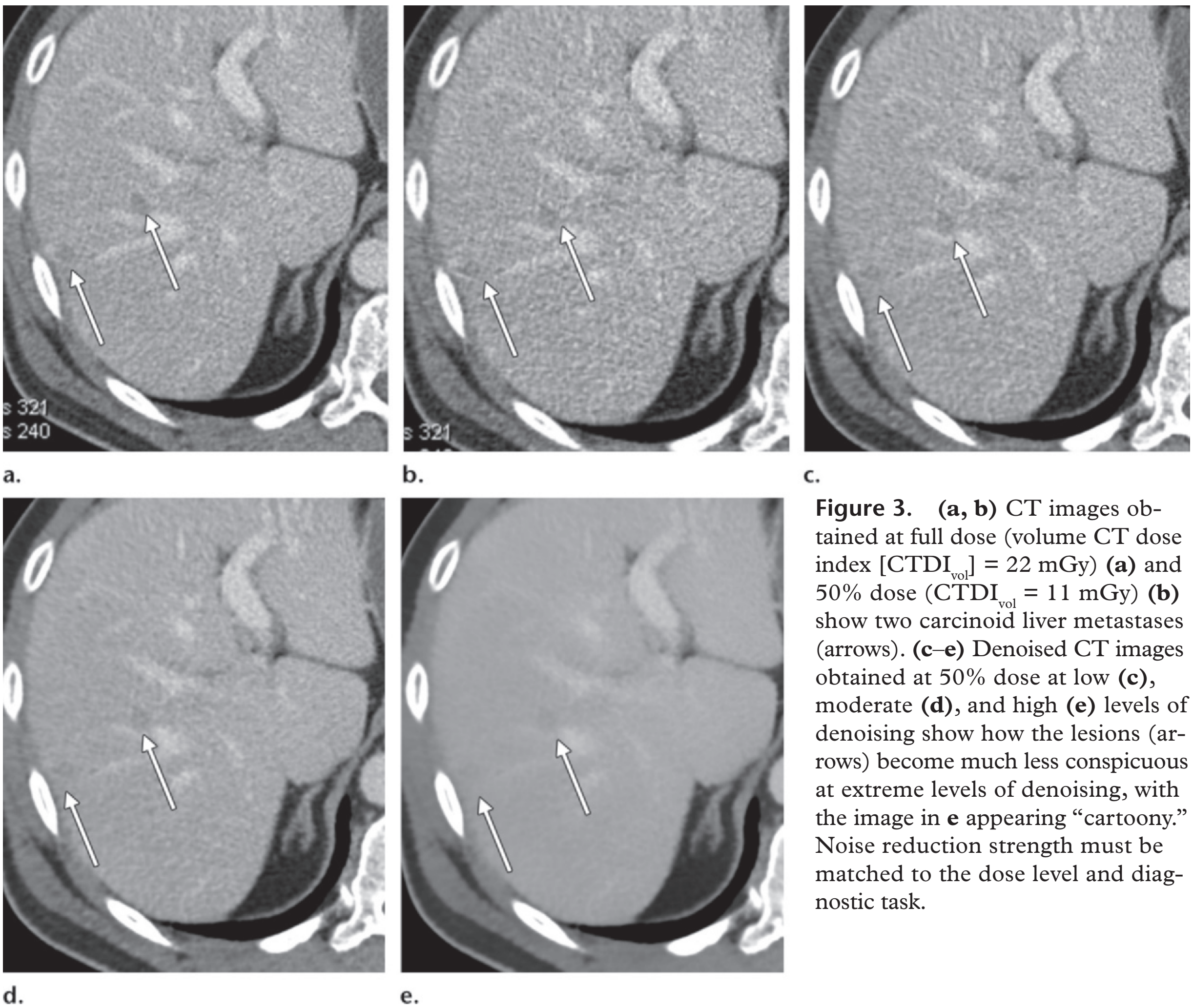

Figure 3. **(a, b)** CT images obtained at full dose (volume CT dose index [$CTDI_{vol}$] = 22 mGy) **(a)** and 50% dose ($CTDI_{vol}$ = 11 mGy) **(b)** show two carcinoid liver metastases (arrows). **(c–e)** Denoised CT images obtained at 50% dose at low **(c)**, moderate **(d)**, and high **(e)** levels of denoising show how the lesions (arrows) become much less conspicuous at extreme levels of denoising, with the image in **e** appearing "cartoony." Noise reduction strength must be matched to the dose level and diagnostic task.

spicuity as increased levels of one type of image space denoising are applied. Image space denoising methods are applied directly to CT images, so that they can be implemented across various CT scanner models from different vendors (10).

Teaching Point

Because a single image space denoising system may service several CT scanners, such denoising can often be implemented at a much lower cost than with other methods and may provide a single denoising solution for small departments with only two or three scanners. Image space filter parameters can usually be set so that the CT images largely retain their "natural" appearance, without the pixelation ("blocky" or cartoony appearance) created by many iterative reconstruction methods, which alter the appearance of CT noise texture

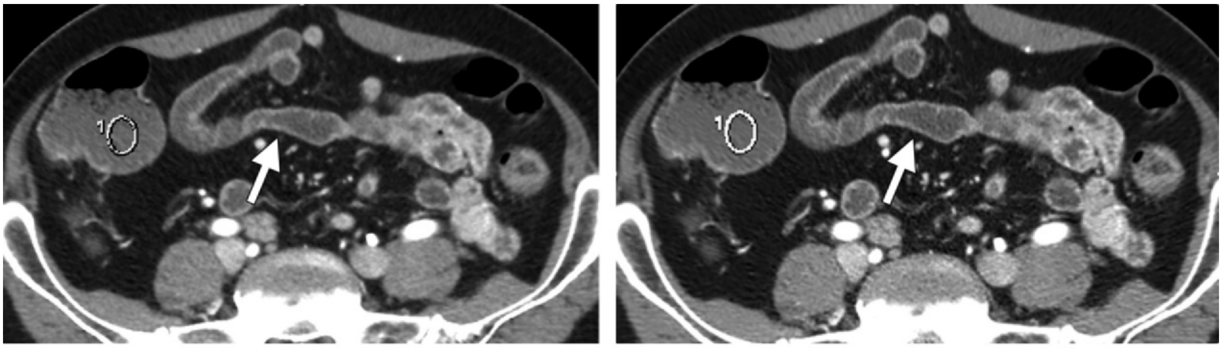

a. b.

Figure 4. Low-dose CT enterographic images with a similar level of noise reduction (verified with CT noise measurement in cecal fluid) obtained with a commercial projection-based denoising method **(a)** and an image-based denoising method **(b)** show an ileal small bowel loop (arrow) whose wall boundaries are slightly blurred with projection-based denoising.

Figure 5. Multifocal hepatocellular carcinomas. **(a)** Late arterial phase contrast-enhanced abdominal CT image obtained at full dose shows two hepatocellular carcinomas (arrows). **(b)** Reconstructed image obtained at 50% dose (80 kV) after projection space denoising shows the carcinomas (arrows) with preserved conspicuity due to noise reduction, with only a slight loss in image sharpness. Noise reduction techniques are often combined with lower-kilovolt imaging to reduce radiation dose and preserve image quality. (Fig 5 reprinted, with permission, from reference 31.)

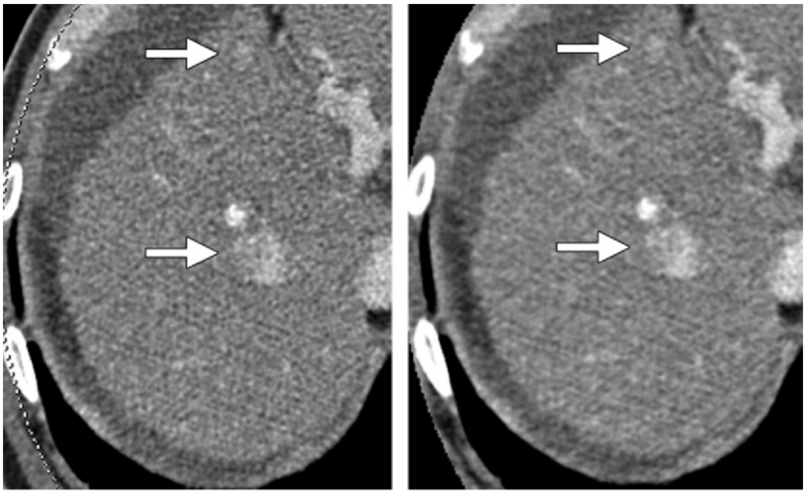

a. b.

(28). Nevertheless, the degree of potential dose reduction with image-based denoising may be limited due to the lack of detailed incorporation of CT system geometry and a statistical model of x-ray photons. Because images must be networked to an image-based denoising system before being sent to a picture archiving and communication system, there is usually a 1–10-minute delay before images can be interpreted, depending on the denoising method and hardware used.

Projection Space Denoising

Projection space denoising is the process of filtering projection space data prior to image reconstruction (17–19,29). These techniques can incorporate photon statistics into the CT data and smooth the data by either optimizing a likelihood function using a statistical noise model (17,18) or applying a nonlinear filter adaptive to the noise (19). Because projection space denoising methods may incorporate system physics and photon statistics, there is the potential for artifact reduction in addition to reduction in image noise. As with other noise reduction methods, loss of spatial resolution and, possibly, loss of low-contrast lesion conspicuity may result if parameters are not carefully optimized (Fig 4). One recently described method of projection space denoising is based on bilateral filtering (19). With this method, as with other methods in this class of techniques, projection space data are smoothed using a weighted average that is based on the spatial proximity and intensity of neighboring pixels, resulting in decreased noise while preserving edge information (19). Studies have demonstrated the ability to substantially reduce the radiation dose in abdominal and hepatic applications by combining lower-kilovolt CT with projection-based techniques to preserve diagnostic image quality and lesion conspicuity (Fig 5) (30–32). Projection space denoising is performed on CT projection data prior to image reconstruction and therefore is generally implemented on a CT scanner's image reconstruction system, which is scanner dependent.

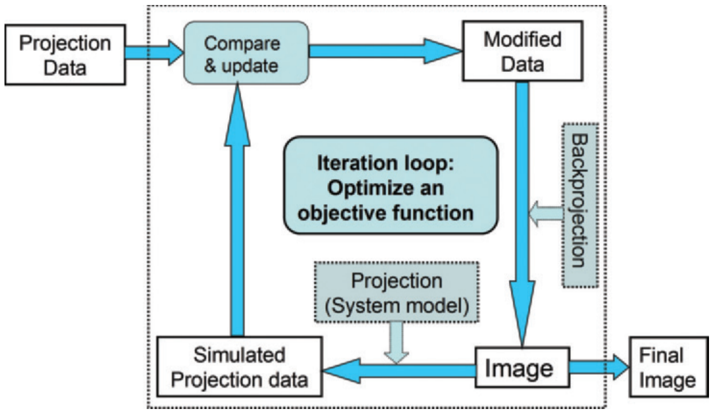

Figure 6. Schematic illustrates the typical iterative reconstruction method. The objective function to be optimized in the iteration loop has many variations, including different statistical models and regularization terms. The system model used during projection can also vary significantly, including a variety of system geometries and x-ray beam transport and detection models.

Consequently, projection space denoising methods are vendor dependent and more costly but do not alter regular clinical workflow compared with analytic FBP when incorporated into a scanner's image reconstruction system.

Iterative Reconstruction

Methods of iterative reconstruction for CT were first developed 20–30 years ago (33,34) but were not applied to clinical CT scanners until recently (25,35). As opposed to traditional analytic FBP-based image reconstruction, in which the images are obtained by filtering the projection data with a reconstruction kernel and then backprojecting the filtered data to the image space, iterative reconstruction calculates the final images using an optimization-based framework (25) in which multiple iterations between projection data space and image space are typically necessary to optimize an objective function. During each iteration, the projection data generated based on a system model are compared with the acquired data and updated. The iteration stops when the objective function is minimized according to convergence criteria (Fig 6). Compared with analytic reconstruction methods, iterative reconstruction can model the system geometry more accurately and incorporate photon statistics and other physical effects such as the x-ray beam spectrum into the objective function. Hence, iterative reconstruction can achieve better noise reduction while maintaining spatial resolution and can reduce some artifacts such as those caused by photon starvation, beam hardening, and metal implants. Like projection space denoising, iterative reconstruction is implemented on a scanner's image reconstruction system, resulting in increased cost (due to separate purchases for each scanner) and, potentially, the inability to adopt this method across an entire fleet of CT scanners (due to older or incompatible scanners). A major disadvantage of iterative reconstruction is that it requires a much longer computational time, especially a "full" version that involves multiple iterations between projection space and image space and incorporates a more accurate system model (25). Hybrid iterative reconstruction methods have also been developed that perform the majority of image noise reduction in image space to increase the speed of image reconstruction so that clinical workflow is unaffected, while performing only projection-backprojection iteration when there is a need to reduce artifacts (36–39). The tradeoffs and potential advantages and disadvantages of hybrid versus full iterative reconstruction in terms of improvement in image quality have yet to be studied. Another potential disadvantage of iterative reconstruction is that it usually changes the noise texture compared with the conventional FBP-based images to which radiologists are accustomed. This altered noise texture can interfere with radiologist satisfaction with images (39). If the diagnostic performance of lower-dose CT images with iterative reconstruction is equal or superior to that of routine-dose CT images with FBP-based reconstruction, the general concern regarding the change in noise texture should not become an obstacle to the widespread deployment of iterative reconstruction on clinical CT scanners (Fig 7). A summary of commonly used noise reduction techniques, including their strengths and limitations, is given in the Table.

Teaching Point

Objective Measures of Image Quality for CT Noise Reduction Methods

Because image noise, noise texture, spatial resolution, and artifacts—not to mention the appearance of organs and lesions—all influence the quality of images, it is important to be able to compare and quantify the changes attributable to different noise reduction techniques. For noise reduction methods involving a nonlinear process, including most of the image space denoising and

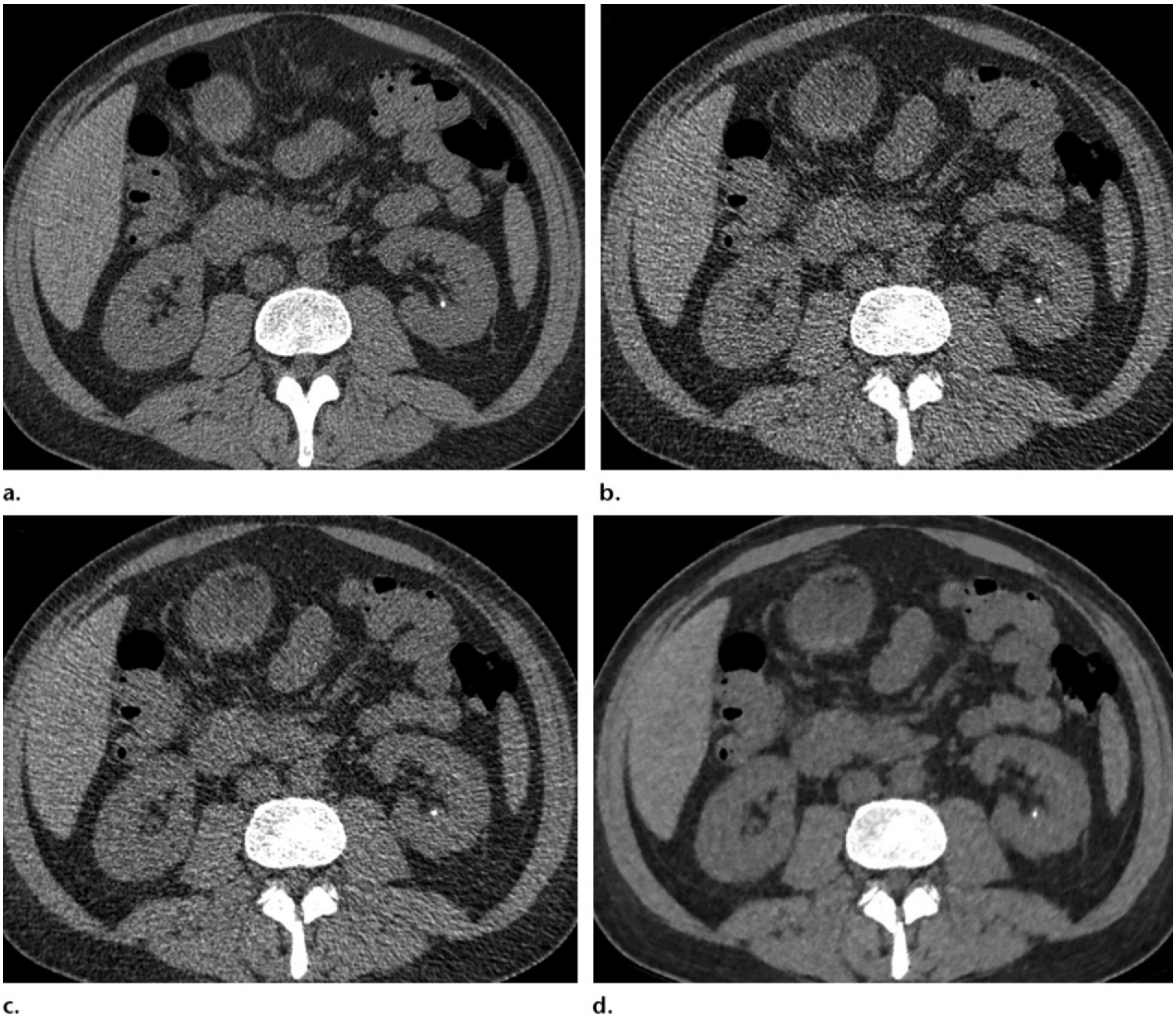

Figure 7. CT images (2-mm thickness) obtained at a standard dose of 7.9 mGy with FBP **(a)** and at 2.8 mGy with FBP **(b)**, adaptive statistical iterative reconstruction (ASIR [GE Healthcare, Waukesha, Wis]) **(c)**, and model-based iterative reconstruction (MBIR [GE Healthcare]) **(d)** show a stone at the tip of the left renal calyx. Note the improved noise reduction and improved stone conspicuity with use of MBIR compared with FBP and ASIR. Improved image quality with iterative reconstruction and other denoising techniques is generally best achieved with use of thinner sections.

iterative reconstruction methods, objective evaluation of image quality is challenging. In the following sections, we describe some image quality metrics that are commonly used to characterize the performance of various noise reduction methods. We pay particular attention to the nonlinearity of noise and spatial resolution properties of noise reduction methods, which results in alterations in spatial resolution and noise that depend on local image characteristics.

Noise Level and Spatial Correlation

Noise level (CT number variation expressed as the standard deviation within a uniform region of interest) is the metric that is most frequently used to describe the noise reduction effect of various methods. However, image noise cannot be fully characterized using noise level alone (Figs 8, 9). Noise spatial correlation is also an important aspect of noise that is closely related to low-contrast object detectability. It may be quantified by analyzing the noise power spectrum (NPS) using an object with a known homogeneous density such as a cylindric water phantom (40). Figure 9 compares the NPS as measured on 3D volumetric images obtained with different noise reduction techniques. Note that when the peak of a curve is farther to the left, the image is smoother and less sharp. The peak frequency of the NPS curve is the spatial frequency at which the NPS curve has the maximum magnitude. The shape and the peak frequency of the NPS curve reflect the loss of low-contrast spatial resolution (Fig 9). Although both iterative reconstruction and FBP kernels can be used to reduce noise, iterative reconstruction results in less reduction of

Commonly Used Noise Reduction Methods and Their Advantages and Disadvantages

Description	Sample Methods	Advantages	Disadvantages
Traditional FBP-based methods	Weighted 3D FBP, AMPR	Fast, directly available on scanners	Treats every ray the same, suboptimal dose efficiency
Image space denoising	SafeCT,* SharpView, aNLM	Fast, needs only reconstructed images, CT vendor independent	Does not incorporate system physics, cannot reduce artifacts
Projection space denoising	Adaptive filtering or iterative denoising in projection data†	Fast, may incorporate complex system physics	Potential loss of spatial resolution if not designed well
Hybrid iterative reconstruction	SAFIRE‡	Noise reduction in image space (for speed), artifact reduction by iteration between image and projection space denoising (for image quality)	May change the noise texture of CT images
Full iterative reconstruction	MBIR	Incorporates system model (both photon statistics and detailed geometry), may potentially reduce both noise and artifacts	Slow, may change the noise texture of CT images

Note.—AIDR3D = 3D adaptive iterative dose reduction (Toshiba Medical Systems, Tokyo, Japan), AMPR = adaptive multiple plane reconstruction (Siemens Medical Solutions, Malvern, Pa), aNLM = adaptive nonlocal means (denoising method), SAFIRE = sinogram-affirmed iterative reconstruction (Siemens).
*Medic Vision Imaging Solutions, Tirat Carmel, Israel.
†ASIR might belong to this category, but no technical details have been published.
‡AIDR3D and iDose (an iterative reconstruction technique developed by Philips Medical Systems, Andover, Mass) might belong to this category, but no technical details have been published.

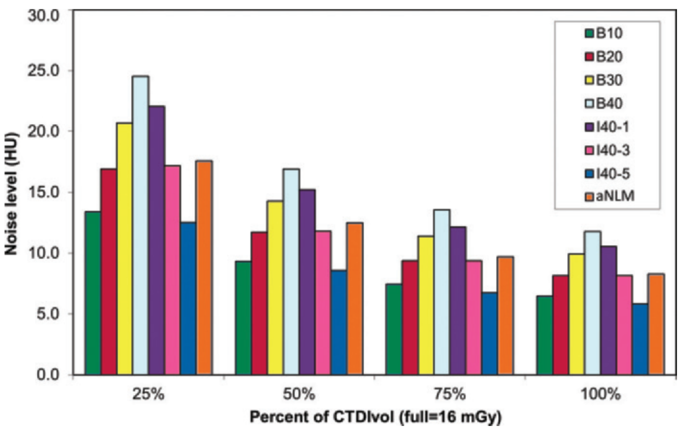

Figure 8. Graph illustrates a comparison of noise levels for four different FBP-based kernels (B40, B30, B20, and B10), three SAFIRE (Siemens) strength settings (I40–1, I40–3, and I40–5 kernels), and one strength setting of an image-based denoising method known as aNLM denoising. Noise level was measured as the standard deviation of CT numbers within a uniform region of interest on CT images of a water phantom 30 cm in diameter. With FBP-based kernels, the noise and sharpness increase as the number increases; conversely, at lower numbers, the noise decreases and the image becomes smoother. With SAFIRE strength settings, image noise decreases with higher settings.

the peak frequency at similar noise levels (Fig 9). This effect corresponds to greater image sharpness. As shown in Figure 10, two images of a uniform water phantom that were obtained with an FBP-based B20 kernel and a SAFIRE (Siemens) I40–3 kernel have almost identical noise levels. However, the "I40–3" image has a finer noise texture and a sharper appearance. A reduced peak frequency of the NPS (ie, a shift of the peak frequency to the left on the NPS curve) corresponds to a blurry appearance of low-contrast objects. Some denoising methods can result in a loss of low-contrast spatial resolution.

Teaching Point

High-Contrast Spatial Resolution

High-contrast spatial resolution at CT is typically evaluated both in-plane and cross-plane (ie, along the z-axis). In-plane spatial resolution can be evaluated qualitatively using the bar patterns found in phantoms such as the American College of Radiology (ACR) accreditation phantom (Fig 11a), or quantitatively by deriving the modulation transfer function (MTF), which is obtained by scanning a high-contrast wire phantom (Fig 11b) (41). Similarly, cross-plane spatial resolution can be assessed qualitatively using the section thickness pattern in the ACR phantom, or quantitatively by measur-

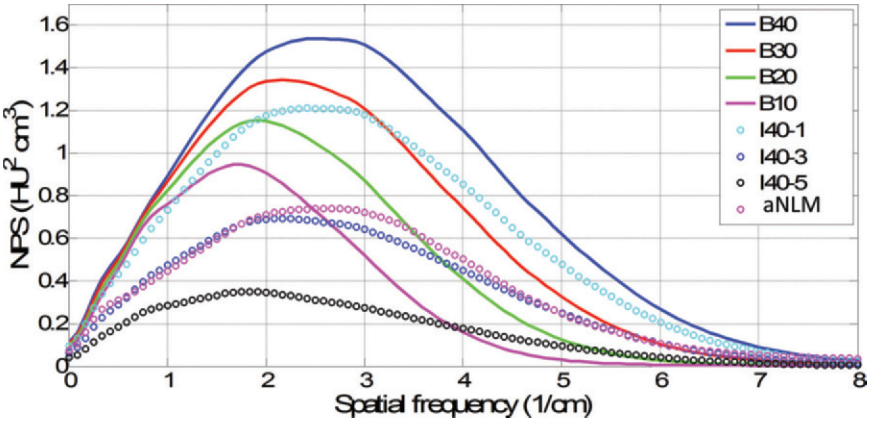

Figure 9. Graph illustrates a comparison of NPS calculated from a three-dimensional (3D) uniform water phantom. The NPS is a more complete descriptor of noise properties than is noise level. The loss of spatial resolution at low contrast can be demonstrated using the shape and peak frequency of the NPS curve. In this example, noise is reduced at the expense of spatial resolution when changing FBP reconstruction kernels (eg, when moving from B40 to B20) (solid lines). With advanced noise reduction methods, the peak frequency (ie, the spatial frequency at which the NPS has the greatest magnitude) shifts to the left to a much lesser extent than with standard FBP kernels, corresponding to a lesser sacrifice of low-contrast spatial resolution and blurriness in noise texture. Advanced noise reduction methods used to create this graph include SAFIRE kernels (I40–1, I40–2, and I40–3 [Siemens]) and aNLM denoising.

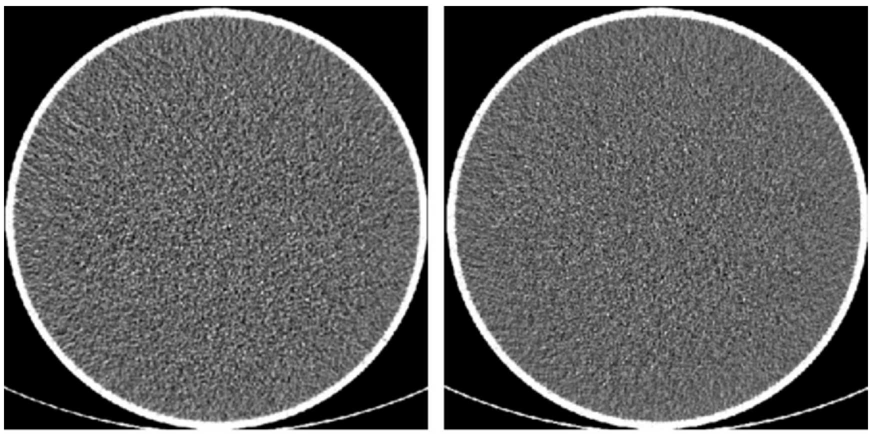

a. b.

Figure 10. Visual comparison of noise texture. Images with similar noise levels obtained with a smooth FBP kernel (B20) **(a)** and iterative reconstruction (I40–3 kernel) **(b)** (standard deviation = 29.1 and 27.7 HU, respectively) show that the image obtained with iterative reconstruction has a sharper appearance, which corresponds to a higher peak frequency in the NPS.

ing the section sensitivity profile (SSP) using a thin foil phantom (Fig 11c) (42). Nonlinear noise reduction methods typically do not sacrifice high-contrast spatial resolution.

Detectability of Low-Contrast Objects

Evaluation of low-contrast object detectability can be undertaken using phantoms (eg, the ACR phantom) containing low-contrast objects. By scanning the phantom at different dose levels and applying the various noise reduction techniques outlined earlier, a direct side-by-side comparison can be made to assess the various techniques in terms of detectability of low-contrast objects. Figure 12 provides a comparison of FBP, SAFIRE (Siemens), and MBIR (GE Healthcare) at 100%, 75%, 50%, and 25% of the full dose ($CTDI_{vol}$ = 16 mGy). Despite an improvement compared with FBP at the same dose level, there is no clear evidence that the visibility of small low-contrast objects with SAFIRE and MBIR at any of the lower dose levels below 12 mGy is comparable to that with FBP at full dose (Fig 12). Therefore, at the contrast level of the low-contrast object in the ACR phantom (~6 HU), the potential dose reduction appears to be very limited. Similarly, in a multireader study involving six radiologists, Baker et al (37) showed that whereas simple metrics such as noise and contrast-to-noise ratio are always improved with iterative reconstruction (regardless of dose), the detectability of low-contrast lesions falls off at lower doses. It should be noted that this type of evaluation is highly subjective and can give only a rough idea as to how much the radiation dose can be reduced at a given low contrast level. More quantitative evaluation of low-contrast lesion detectability for iterative reconstruction using task-based model observers is currently an area of active research (43), as are observer studies (44,45).

Nonlinearity of Noise Reduction Methods: Special Considerations

In contrast to conventional analytic FBP-based reconstruction methods, spatial resolution in

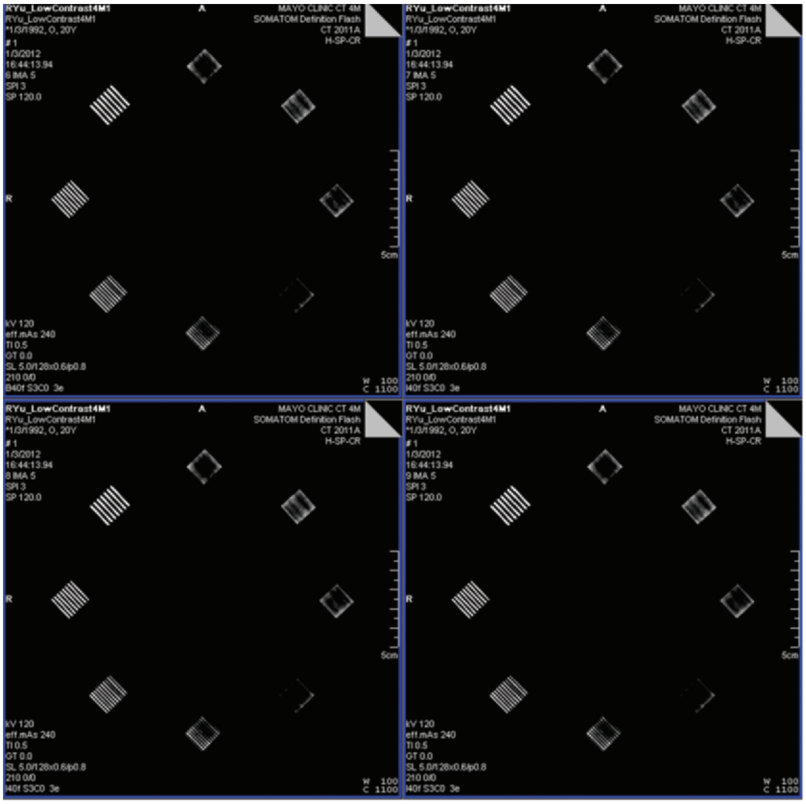

a.

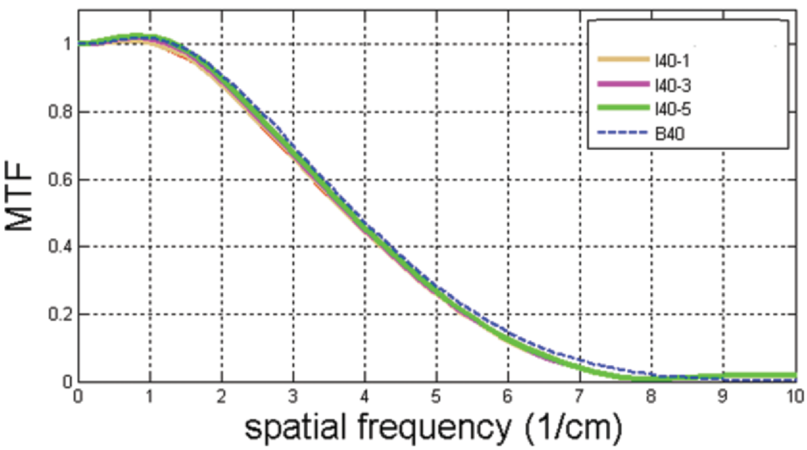

b.

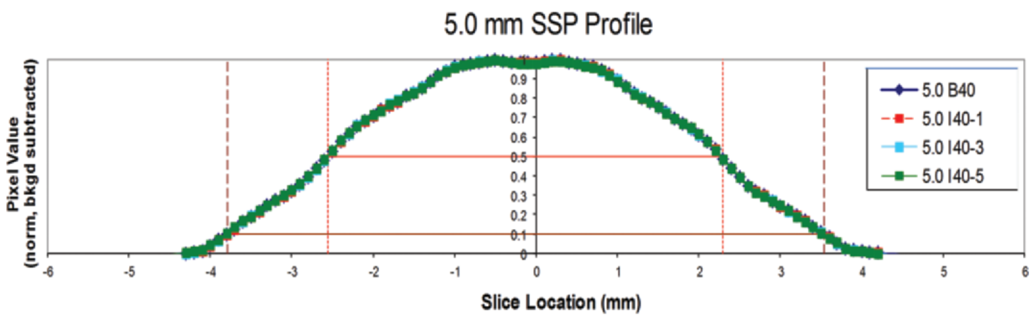

c.

Figure 11. **(a)** Images show the qualitative descriptor of in-plane high-contrast spatial resolution using the bar pattern in an ACR phantom. **(b)** Graph illustrates the quantitative descriptor of in-plane spatial resolution as the MTF, shown here for a routine reconstruction kernel (B40) and SAFIRE kernels (I40 with three different strength settings [Siemens]). **(c)** Graph illustrates how the SSP is used to measure spatial resolution in the z-axis direction. Note the preserved high-contrast spatial resolution with SAFIRE despite a reduction in image noise. *bkgd* = background.

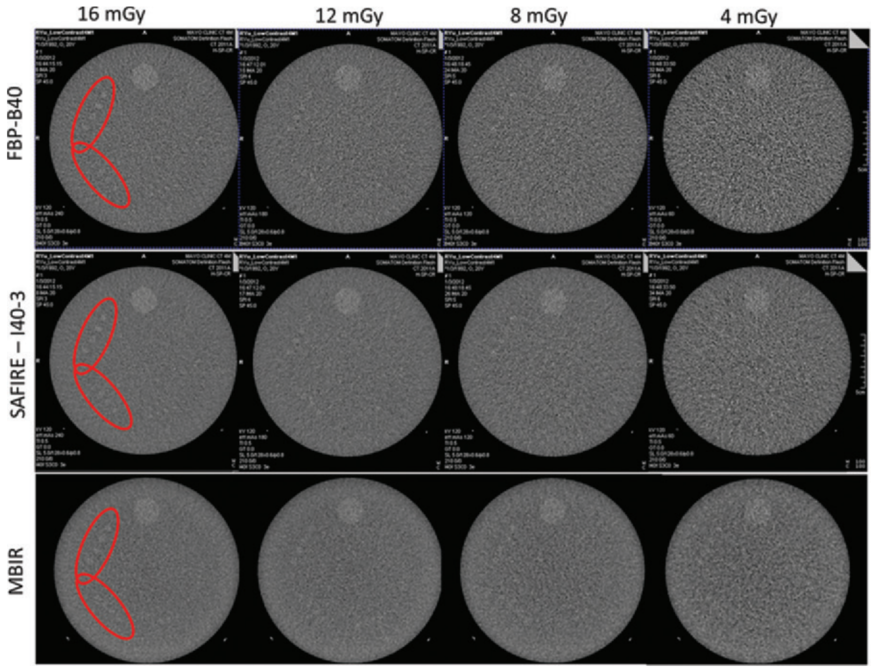

Figure 12. Images of the low-contrast module of the ACR phantom obtained at multiple dose levels (16, 12, 8, and 4 mGy) and reconstructed with an FBP kernel (B40) and two iterative reconstruction methods (SAFIRE [I40–3]) and MBIR) from two different manufacturers (Siemens and GE Healthcare). Both iterative reconstruction methods lower the noise level and improve the visibility of the small low-contrast rods (ellipses on the 16-mGy images) at each dose level. However, a comparison of the visibility of the rods at different dose levels reveals that neither iterative reconstruction method restores the visibility of the rods at lower doses to the level seen at full dose.

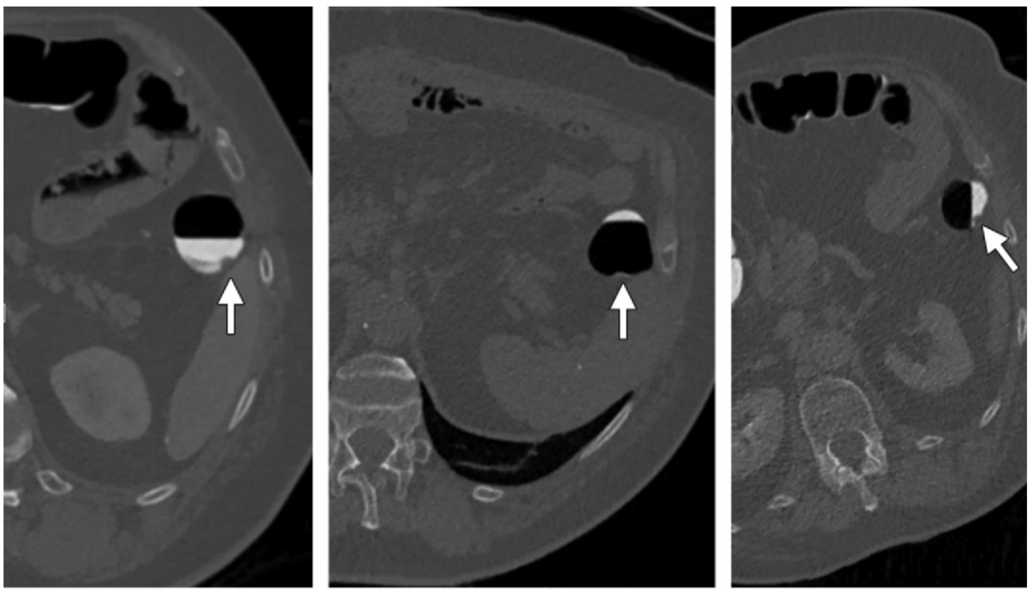

a. b. c.

Figure 13. **(a)** Contrast-enhanced 1-mm-thick CT colonographic image ($CTDI_{vol}$ = 20 mGy) obtained with the patient supine for the purpose of ruling out liver metastases demonstrates a 0.7-cm polyp (tubular adenoma) (arrow) in the descending colon. **(b, c)** On contrast-enhanced 1-mm-thick CT colonographic images obtained with SAFIRE (Siemens) with the patient prone ($CTDI_{vol}$ = 3.52 mGy) **(b)** and in the decubitus position ($CTDI_{vol}$ = 1.39 mGy) **(c)**, the polyp is still visible despite a dose reduction of over 80% and 93%, respectively. This is due to the high-contrast diagnostic task (ie, differentiating a polyp from air or contrast material).

iterative reconstruction and other nonlinear noise reduction methods is dependent on the contrast level of the lesion (46). Nonlinear noise reduction methods can typically achieve a significant reduction in noise level without degrading high-contrast spatial resolution. For this reason, if only the amount of noise reduction is taken into account, it can appear that most nonlinear noise reduction methods can achieve at least 50% dose reduction. For example, as shown in Figure 8, the noise level at a 25% dose level with a higher strength of iterative reconstruction (the I40–5 kernel) and the noise level at a 50% dose level with a moderate strength of iterative reconstruction (the I40–3

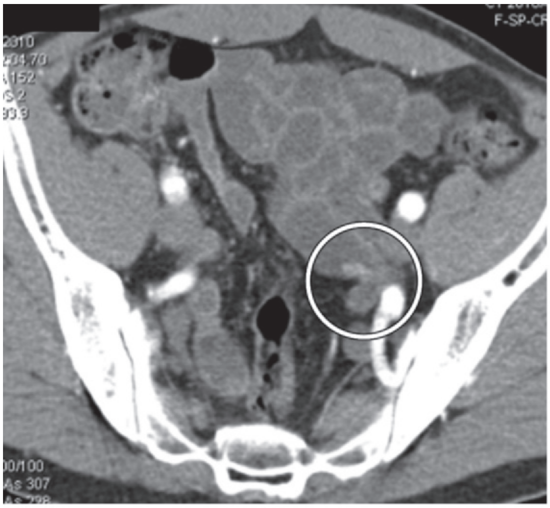

a.

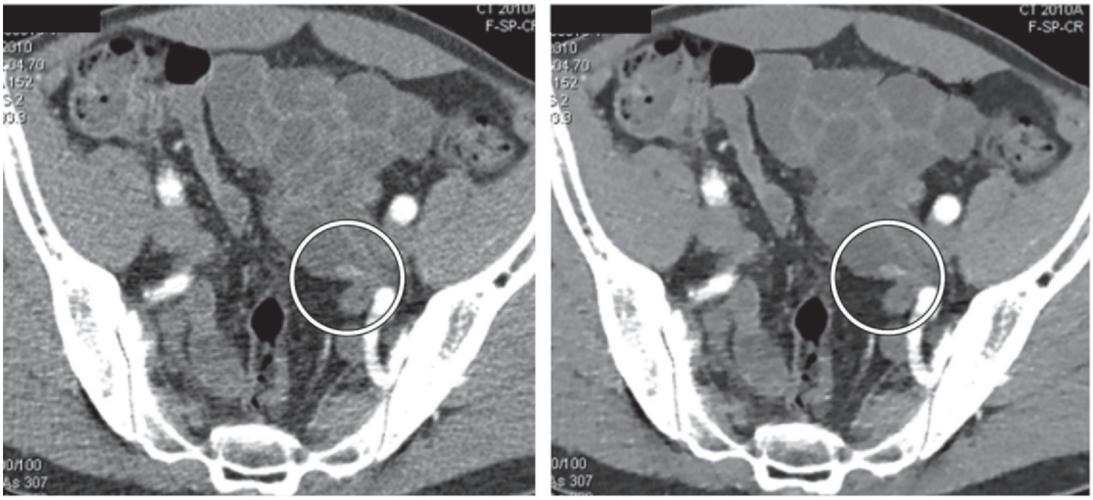

b. c.

Figure 14. Triple-phase 2-mm-thick CT enterographic images obtained at routine dose ($CTDI_{vol}$ = 12 mGy) with FBP **(a)** and at 30% dose ($CTDI_{vol}$ = 3.6 mGy) with FBP **(b)** and SAFIRE (Siemens) **(c)** all show a small, hyperattenuating ileal mass (circle). Diagnostic tasks requiring differentiation of large contrast differences (ie, "high-contrast" tasks) permit marked reductions in radiation dose.

kernel) are both similar to that at full dose with the regular FBP kernel (B40). The fact that the high-contrast resolution, measured as the MTF (in-plane) or SSP (cross-plane) (Fig 11), remains the same after applying the iterative reconstruction method suggests that radiation dose can be reduced by 50% using the I40–3 kernel and by 75% using the I40–5 kernel. If contrast-to-noise ratio is used as the criterion, the same dose reduction results would be obtained as with use of noise level as the criterion, since contrast does not change for these different reconstruction methods. However, this amount of radiation dose reduction is not achievable if one compares the detectability of low-contrast objects at different radiation dose levels for different reconstruction methods (Fig 12). In addition, at low contrast levels, a loss of sharpness can usually be associated with noise reduction, which can be seen in the change of noise texture and quantified by the shape and the reduction of the peak frequency of the NPS curve. Therefore, the nonlinearity of the noise reduction methods makes the dose reduction potential highly dependent on the contrast level of the target object. Consequently, for diagnostic tasks involving high-contrast structures, the dose reduction potential is usually higher than for those tasks involving low-contrast lesions.

Clinical Application of Nonlinear Noise Reduction Methods

As seen in the aforementioned examples involving the imaging of phantoms, iterative reconstruction and nonlinear denoising may maintain high-contrast spatial resolution while simultaneously reducing image noise. This is especially true when there is high intrinsic contrast between the lesion of interest and adjacent tissues, as at CT colonography, CT for renal calculi, and CT enterography for the evaluation of Crohn disease (Figs 7, 13, 14) (47). Consequently, the potential for dose reduction for these high-contrast tasks is high.

Teaching Point

Conversely, because of the sacrifice of low-contrast spatial resolution with noise reduction

Figure 15. (a) FBP CT image obtained at routine dose ($CTDI_{vol}$ = 10.4 mGy) shows a colon cancer metastasis (arrow) in the medial segment of the liver. (b–e) CT images obtained at 25% dose with image-based aNLM denoising (b) and SAFIRE (Siemens) (c) and at 10% dose with aNLM denoising (d) and SAFIRE (e). The lesion (arrow) is visible down to the 25% dose level but is not clearly visible with either noise reduction method at the 10% dose level.

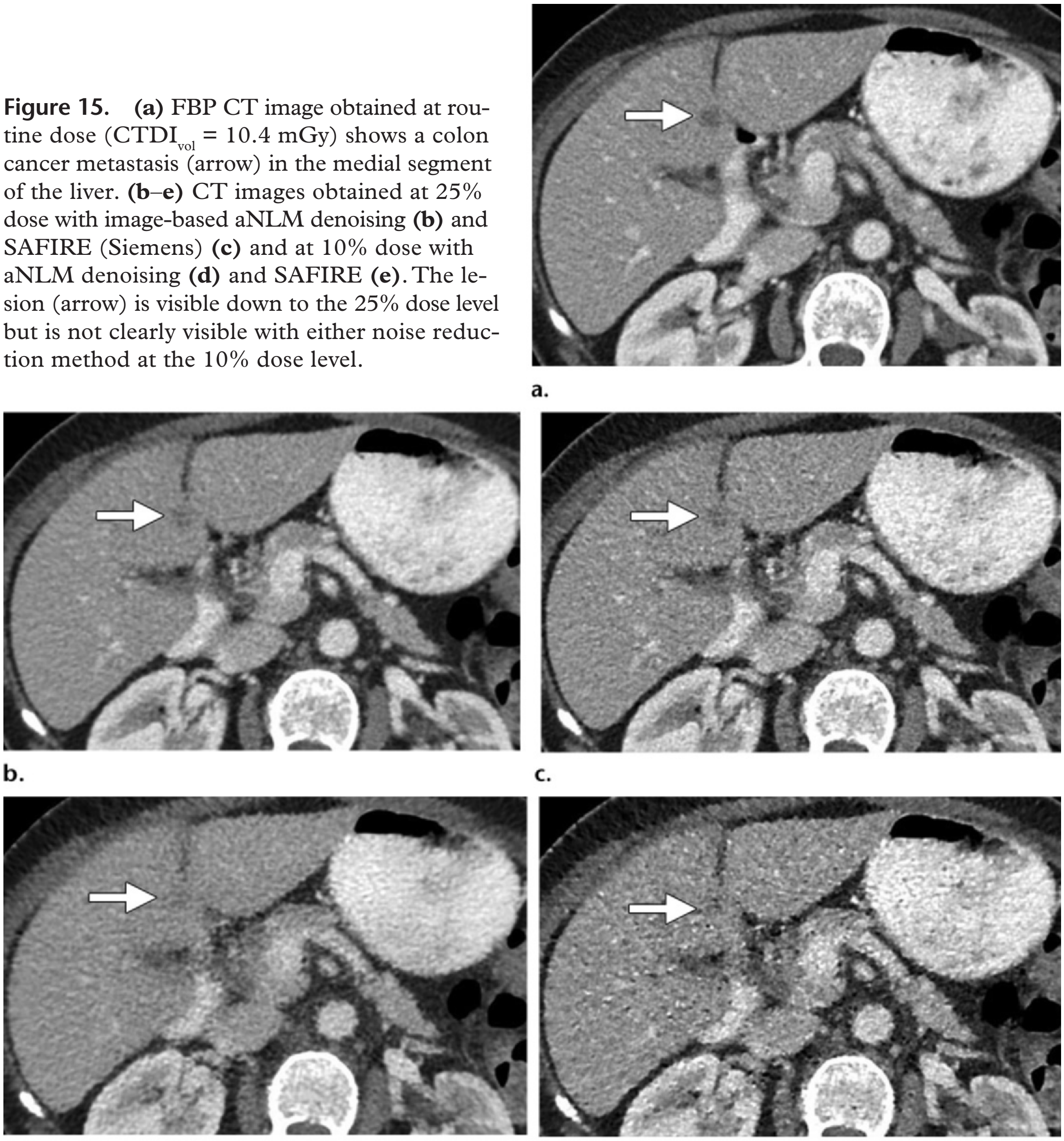

a. b. c. d. e.

techniques, clinical situations in which there is low intrinsic contrast between the lesion and normal tissue (eg, at hepatic, pancreatic, or neurologic CT) will likely permit less dose reduction so as to maintain clinically acceptable image quality and diagnostic performance (Figs 15, 16) (47).

Conclusion

Multiple institutions have shown that careful integration of noise reduction strategies into clinical practice can make a significant contribution to lowering the radiation dose (31,35,48–51). To preserve the diagnostic benefit of CT (and to ensure accuracy of detection and diagnosis), careful optimization is needed when adopting these methods. Special attention must be paid to the diagnostic task required in each patient. Potential dose reduction using noise reduction methods is dependent on lesion-to-background contrast and the anatomy of interest. High-contrast tasks such as CT colonography, renal stone detection, and CT enterography will permit large reductions in radiation dose. Low-contrast tasks such as the detection of liver metastasis will permit smaller reductions in radiation dose. Methods are needed for quantitating contrast-dependent spatial resolution, conducting observer performance studies for a variety of diagnostic tasks (and developing tools to facilitate the rapid completion of these tasks), and predicting the lowest dose that will allow adequate performance on specific CT systems. The full impact of noise reduction techniques on radiation dose and radiologist performance is in the early phases of realization, with great potential to benefit patients by decreasing the radiation dose they receive while undergoing CT.

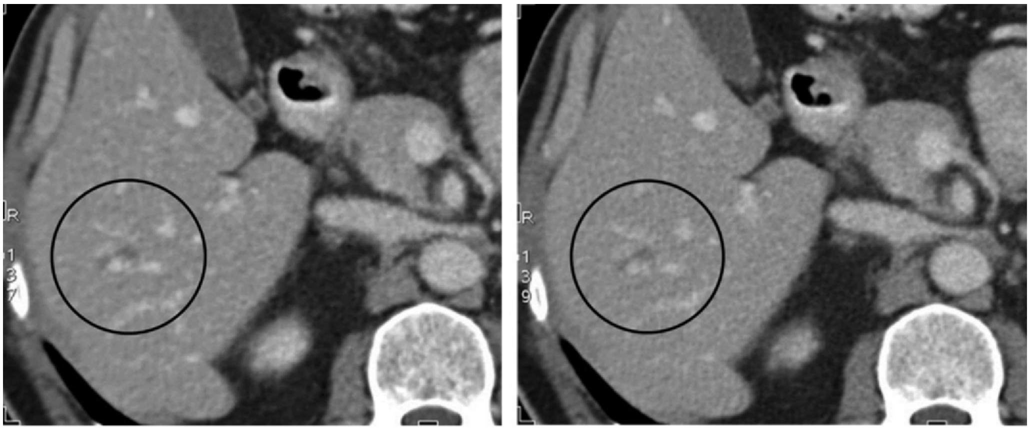

a. b.

Figure 16. Comparison of two image-based denoising methods. CT images demonstrate nonlinearity of low-contrast spatial resolution and high contrast signal. Note the improved conspicuity of peripheral globular enhancement within a hemangioma (circle) in **a** compared with **b**, despite similar reductions in noise, and slightly decreased image sharpness and coarser noise texture in **a**.

***Disclosures of Conflicts of Interest.*—A.K.H.:** *Related financial activities:* research agreement with GE Healthcare. *Other financial activities:* licensure for CT colonography (GE Healthcare). **A.M.:** *Related financial activities:* none. *Other financial activities:* patents filed for a system and method for controlling radiation dose in radiologic applications and for projection space denoising with bilateral filtering in CT. **C.H.M.:** *Related financial activities:* none. *Other financial activities:* grant from Siemens Medical Solutions, patent filed for aNLM denoising of CT images. **D.J.B.:** *Related financial activities:* patent filed on some aspects of the algorithm. *Other financial activities:* none. **J.G.F.:** *Related financial activities:* none. *Other financial activities:* grant from Siemens Medical Solutions, patents for projection space and nonlocal means denoising of CT images, patent filed for aNLM denoising of CT images.

References

1. National Council on Radiation Protection and Measurements. Ionizing radiation exposure of the population of the United States. Report No. 160. Bethesda, Md: National Council on Radiation Protection and Measurements, 2009.
2. Smith-Bindman R, Miglioretti DL, Johnson E, et al. Use of diagnostic imaging studies and associated radiation exposure for patients enrolled in large integrated health care systems, 1996–2010. JAMA 2012;307(22):2400–2409.
3. Brenner DJ, Hall EJ. Computed tomography: an increasing source of radiation exposure. N Engl J Med 2007;357(22):2277–2284.
4. Smith-Bindman R, Lipson J, Marcus R, et al. Radiation dose associated with common computed tomography examinations and the associated lifetime attributable risk of cancer. Arch Intern Med 2009; 169(22):2078–2086.
5. Linet MS, Slovis TL, Miller DL, et al. Cancer risks associated with external radiation from diagnostic imaging procedures. CA Cancer J Clin 2012;62:75–100.
6. Pearce MS, Salotti JA, Little MP, et al. Radiation exposure from CT scans in childhood and subsequent risk of leukaemia and brain tumours: a retrospective cohort study. Lancet 2012;380(9840):499–505.
7. McCollough CH, Guimarães L, Fletcher JG. In defense of body CT. AJR Am J Roentgenol 2009;193 (1):28–39.
8. Yu L, Liu X, Leng S, et al. Radiation dose reduction in computed tomography: techniques and future perspective. Imaging Med 2009;1(1):65–84.
9. McCollough CH, Primak AN, Braun N, Kofler J, Yu L, Christner J. Strategies for reducing radiation dose in CT. Radiol Clin North Am 2009;47(1):27–40.
10. Del Gaizo AJ, Fletcher JG, Yu L, et al. Reducing radiation dose in CT enterography. RadioGraphics 2013;33(4):1109–1124.
11. Kak A, Slaney M. Principles of computed tomographic imaging. Philadelphia, Pa: Society for Industrial and Applied Mathematics, 1987.
12. Kim K, Kim YH, Kim SY, et al. Low-dose abdominal CT for evaluating suspected appendicitis. N Engl J Med 2012;366(17):1596–1605.
13. Allen BC, Baker ME, Einstein DM, et al. Effect of altering automatic exposure control settings and quality reference mAs on radiation dose, image quality, and diagnostic efficacy in MDCT enterography of active inflammatory Crohn's disease. AJR Am J Roentgenol 2010;195(1):89–100.
14. Kambadakone AR, Prakash P, Hahn PF, Sahani DV. Low-dose CT examinations in Crohn's disease: impact on image quality, diagnostic performance, and radiation dose. AJR Am J Roentgenol 2010;195(1):78–88.
15. Tack D, Bohy P, Perlot I, et al. Suspected acute colon diverticulitis: imaging with low-dose unenhanced multi–detector row CT. Radiology 2005;237(1):189–196.
16. Seo H, Lee KH, Kim HJ, et al. Diagnosis of acute appendicitis with sliding slab ray-sum interpretation of low-dose unenhanced CT and standard-dose i.v. contrast-enhanced CT scans. AJR Am J Roentgenol 2009;193(1):96–105.
17. Wang J, Li T, Lu H, Liang Z. Penalized weighted least-squares approach to sinogram noise reduction and image reconstruction for low-dose X-ray computed tomography. IEEE Trans Med Imaging 2006;25(10):1272–1283.
18. La Rivière PJ, Bian J, Vargas PA. Penalized-likelihood sinogram restoration for computed tomography. IEEE Trans Med Imaging 2006;25(8):1022–1036.
19. Manduca A, Yu L, Trzasko JD, et al. Projection space denoising with bilateral filtering and CT noise modeling for dose reduction in CT. Med Phys 2009;36(11):4911–4919.
20. Bai M, Chen J, Raupach R, Suess C, Tao Y, Peng M. Effect of nonlinear three-dimensional optimized

reconstruction algorithm filter on image quality and radiation dose: validation on phantoms. Med Phys 2009;36 (1):95–97.
21. Singh S, Kalra MK, Forsberg A, Gilman MD, Shepard JO, Blake MA. Integration of 2D adaptive algorithms in routine clinical workflow for reducing CT radiation dose [abstr]. In: Radiological Society of North America Scientific Assembly and Annual Meeting Program. Oak Brook, Ill: Radiological Society of North America, 2009; 1079.
22. Lange K, Fessler JA. Globally convergent algorithms for maximum a posteriori transmission tomography. IEEE Trans Image Process 1995;4(10):1430–1438.
23. Nuyts J, De Man B, Dupont P, Defrise M, Suetens P, Mortelmans L. Iterative reconstruction for helical CT: a simulation study. Phys Med Biol 1998;43(4):729–737.
24. Elbakri IA, Fessler JA. Statistical image reconstruction for polyenergetic X-ray computed tomography. IEEE Trans Med Imaging 2002;21(2):89–99.
25. Thibault JB, Sauer KD, Bouman CA, Hsieh J. A three-dimensional statistical approach to improved image quality for multislice helical CT. Med Phys 2007;34 (11):4526–4544.
26. Szucs-Farkas Z, Bensler S, Torrente JC, Cullmann JL, Vock P, Schindera ST. Nonlinear three-dimensional noise filter with low-dose CT angiography: effect on the detection of small high-contrast objects in a phantom model. Radiology 2011;258(1):261–269.
27. Bittencourt MS, Schmidt B, Seltmann M, et al. Iterative reconstruction in image space (IRIS) in cardiac computed tomography: initial experience. Int J Cardiovasc Imaging 2011;27(7):1081–1087.
28. Froemming AT, Kawashima A, Takahashi N, et al. Individualized kV selection and tube current reduction in excretory phase computed tomography urography: potential for radiation dose reduction and the contribution of iterative reconstruction to image quality. J Comput Assist Tomogr 2013;37(4):551–559.
29. Hsieh J. Adaptive streak artifact reduction in computed tomography resulting from excessive x-ray photon noise. Med Phys 1998;25(11):2139–2147.
30. Guimarães LS, Fletcher JG, Yu L, et al. Feasibility of dose reduction using novel denoising techniques for low kV (80 kV) CT enterography: optimization and validation. Acad Radiol 2010;17(10):1203–1210.
31. Ehman EC, Guimarães LS, Fidler JL, et al. Noise reduction to decrease radiation dose and improve conspicuity of hepatic lesions at contrast-enhanced 80-kV hepatic CT using projection space denoising. AJR Am J Roentgenol 2012;198(2):405–411.
32. Kaza RK, Platt JF, Al-Hawary MM, Wasnik A, Liu PS, Pandya A. CT enterography at 80 kVp with adaptive statistical iterative reconstruction versus at 120 kVp with standard reconstruction: image quality, diagnostic adequacy, and dose reduction. AJR Am J Roentgenol 2012; 198(5):1084–1092.
33. Lange K, Carson R. EM reconstruction algorithms for emission and transmission tomography. J Comput Assist Tomogr 1984;8(2):306–316.
34. Fessler JA. Penalized weighted least-squares image reconstruction for positron emission tomography. IEEE Trans Med Imaging 1994;13(2):290–300.
35. Sagara Y, Hara AK, Pavlicek W, Silva AC, Paden RG, Wu Q. Abdominal CT: comparison of low-dose CT with adaptive statistical iterative reconstruction and routine-dose CT with filtered back projection in 53 patients. AJR Am J Roentgenol 2010;195(3):713–719.
36. Bruder H, Kachelriess M, Schaller S, Stierstorfer K, Flohr T. Single-slice rebinning reconstruction in spiral cone-beam computed tomography. IEEE Trans Med Imaging 2000;19(9):873–887.
37. Baker ME, Dong F, Primak A, et al. Contrast-to-noise ratio and low-contrast object resolution on full- and low-dose MDCT: SAFIRE versus filtered back projection in a low-contrast object phantom and in the liver. AJR Am J Roentgenol 2012;199(1):8–18.
38. Fletcher JG, Grant KL, Fidler JL, et al. Validation of dual-source single-tube reconstruction as a method to obtain half-dose images to evaluate radiation dose and noise reduction: phantom and human assessment using CT colonography and sinogram-affirmed iterative reconstruction (SAFIRE). J Comput Assist Tomogr 2012;36(5):560–569.
39. Fletcher JG, Krueger WR, Hough DM, et al. Pilot study of detection, radiologist confidence and image quality with sinogram-affirmed iterative reconstruction at half-routine dose level. J Comput Assist Tomogr 2013;37(2): 203–211.
40. Siewerdsen JH, Cunningham IA, Jaffray DA. A framework for noise-power spectrum analysis of multidimensional images. Med Phys 2002;29(11):2655–2671.
41. Boone JM. Determination of the presampled MTF in computed tomography. Med Phys 2001;28(3):356–360.
42. Kopp AF, Klingenbeck-Regn K, Heuschmid M, et al. Multislice computed tomography: basic principles and clinical applications. Electromedica 2000;68(2):94–105. http://www.uc.pt/en/fmuc/phdhs/Courses/biomedicalimaging/CT_Article2.pdf.
43. Yu L, Leng S, Chen L, Kofler JM, Carter RE, McCollough CH. Prediction of human observer performance in a 2-alternative forced choice low-contrast detection task using channelized Hotelling observer: impact of radiation dose and reconstruction algorithms. Med Phys 2013;40(4):041908.
44. Pickhardt PJ, Lubner MG, Kim DH, et al. Abdominal CT with model-based iterative reconstruction (MBIR): initial results of a prospective trial comparing ultralow-dose with standard-dose imaging. AJR Am J Roentgenol 2012;199(6):1266–1274.
45. McCollough CH, Leng S, Sunnegardh J, et al. Spatial resolution improvement and dose reduction potential for inner ear CT imaging using a z-axis deconvolution technique. Med Phys 2013;40(6):061904.
46. Evans JD, Politte DG, Whiting BR, O'Sullivan JA, Williamson JF. Effect of contrast magnitude and resolution metric on noise-resolution tradeoffs in x-ray CT imaging: a comparison of non-quadratic penalized alternating minimization and filtered backprojection algorithms. Proc SPIE 2011;7961:79612C.
47. Fletcher JG, Kofler JM, Coburn JA, Bruining DH, McCollough CH. Perspective on radiation risk in CT imaging. Abdom Imaging 2013;38(1):22–31.
48. Hara AK, Paden RG, Silva AC, Kujak JL, Lawder HJ, Pavlicek W. Iterative reconstruction technique for reducing body radiation dose at CT: feasibility study. AJR Am J Roentgenol 2009;193(3):764–771.
49. Prakash P, Kalra MK, Kambadakone AK, et al. Reducing abdominal CT radiation dose with adaptive statistical iterative reconstruction technique. Invest Radiol 2010;45(4):202–210.
50. Kalra MK, Woisetschläger M, Dahlström N, et al. Radiation dose reduction with sinogram affirmed iterative reconstruction technique for abdominal computed tomography. J Comput Assist Tomogr 2012;36(3): 339–346.
51. Singh S, Kalra MK, Hsieh J, et al. Abdominal CT: comparison of adaptive statistical iterative and filtered back projection reconstruction techniques. Radiology 2010;257(2):373–383.

RadioGraphics

Methods for Clinical Evaluation of Noise Reduction Techniques in Abdominopelvic CT

Eric C. Ehman, MD • Lifeng Yu, PhD • Armando Manduca, PhD • Amy K. Hara, MD • Maria M. Shiung, BA • Dayna Jondal, BA • David S. Lake, MS • Robert G. Paden, MS • Daniel J. Blezek, PhD • Michael R. Bruesewitz, RT • Cynthia H. McCollough, PhD • David M. Hough, MD • Joel G. Fletcher, MD

RadioGraphics 2014; 34:849–862 • **Published online** 10.1148/rg.344135128 • **Content Codes:** CT GI PH QA

Page 850

For many diagnostic tasks in abdominal CT, noisy low-dose images can be readily interpreted by radiologists without any adverse effects on diagnostic performance.

Pages 851–852

Because a single image space denoising system may service several CT scanners, such denoising can often be implemented at a much lower cost than with other methods and may provide a single denoising solution for small departments with only two or three scanners. Image space filter parameters can usually be set so that the CT images largely retain their "natural" appearance, without the pixelation ("blocky" or cartoony appearance) created by many iterative reconstruction methods, which alter the appearance of CT noise texture.

Page 853

Iterative reconstruction can achieve better noise reduction while maintaining spatial resolution and can reduce some artifacts such as those caused by photon starvation, beam hardening, and metal implants.

Page 855

A reduced peak frequency of the NPS (ie, a shift of the peak frequency to the left on the NPS curve) corresponds to a blurry appearance of low-contrast objects. Some denoising methods can result in a loss of low-contrast spatial resolution.

Page 860

Because of the sacrifice of low-contrast spatial resolution with noise reduction techniques, clinical situations in which there is low intrinsic contrast between the lesion and normal tissue (eg, at hepatic, pancreatic, or neurologic CT) will likely permit less dose reduction so as to maintain clinically acceptable image quality and diagnostic performance.